Net shape formed spiral and helical piezoelectric actuators

D. H. PEARCE
IRC in Materials, University of Birmingham, Birmingham, UK

K. A. SEFFEN
University of Manchester Institute of Science and Technology, Manchester, UK

T. W. BUTTON
IRC in Materials, University of Birmingham, Birmingham, UK
E-mail: t.w.button@bham.ac.uk

Piezoelectric actuators tend to be made from relatively simple shapes such as blocks, plates and beams. These shapes allow for a range of displacements from key actuation modes but, in order to expand this range, complex structures are required that cannot be made via conventional means. This study presents a novel manufacturing method for such structures using a green ceramic tape lamination process followed by plastic deformation. Furthermore, a helix and a spiral are introduced as examples of initially curved structures. Their actuated behaviour is described by simple but effective models in terms of the standard linear piezoelectric coefficients and is compared to experiments. It is shown that displacements are produced by actuation mechanisms not previously reported in the literature.

1. Introduction

The piezoelectric phenomenon has been known for over a century, and it describes the actuation of strains in a material subject to an electric field, and vice versa. The most common artificial piezoelectrics derive from ferroelectric polycrystalline ceramics such as lead zirconate titanate (PZT). Over the past few decades, basic shapes have been manufactured using conventional ceramic processing methods, and their performance during actuation has been fully realised and exploited [1]. The actuation "modes" are readily expressed in terms of piezoelectric coefficients, d_{xy}, for each type of actuator: x refers to the direction of the applied field and y is the axis of effective strain. For simplicity, actuators that utilise a travelling wave or stepping action, as in piezoelectric motors, are not considered here.

The d_{33} coefficient is used to describe the simplest form of direct actuation, as in a solid block or tube, where the applied field is parallel to the axis of strain. These structures are monolithic but more sophisticated set-ups utilise multiple connected layers to reduce the electric field for a given strain. A recent application is in the direct injector systems in diesel and petrol engines.

The d_{31} coefficient applies to strains orthogonal to the field. Even though d_{31} is smaller in magnitude than d_{33}, it is possible to extract increasingly larger displacements in one of three ways. Practically, it is simple to make the width of section larger than the depth, and the rearrangement resembles a flat strip or plate with the 3-axis as through the thickness and the 1-axis as longitudinal. Thus, the strains integrate over a greater length to produce more displacement. Second, this strip can be bonded to a similar sized strip of different and inactive material resulting a "Unimorph" structure. During actuation, a differential strain profile across the depth gives rise to out-of-plane bending displacements. Finally, and most common, a "bimorph" structure uses two connected piezoelectric strips with a common middle electrode; the actuation strains in each layer are in opposite senses to yield a larger curvature and, hence, displacements. Co-fired bimorphs are commonly made, and many have multiple layers so that applied voltage may be reduced. Actuators with bimorphs have high-resolution capabilities yet generate displacements of several millimetres and can support tip forces up to one Newton. A common application is in scanning VCR heads, where a piezoelectric bimorph compensates for the position of the reading head at different play speeds [2].

The third important coefficient is d_{15}, which couples the applied field to shear strains. This actuation mode is least used, as it requires the electric field to be applied normal to the direction of polarisation and introduces practical difficulties. However, d_{15} is the largest of all coefficients and the potential actuation returns outweigh the inconvenience. This mode is used in various niche market applications, such as accelerometers and, more recently, in fast response printing heads.

The piezoelectric structures described above, along with other planar and cylindrical forms, are made using conventional ceramic technology including dry powder pressing, extrusion, tape casting and post-sintering or green machining. It would appear that, even with these simple shapes, an extensive range of actuation modes is possible, if not fully exhausted. However, this is not the case. Indeed, several theoretical designs claim to generate large linear and rotational displacements using various structures based on helices, spirals and other curved forms [3, 4]. These have suffered from being impractical to manufacture or from having inherent inefficiencies in their electromechanical behaviour. Nonetheless, the principles therein have motivated this study towards an improved family of actuators of the same geometric type.

Each actuator of this study is a co-fired bimorph in which the electrodes have negligible thickness compared to the ceramic layers. In a straight bimorph, the longitudinal strain profile across the depth can be extracted from knowledge of a bimetallic strip performance [5]. Simply interchanging the temperature strain coefficient and ambient temperature for the d_{31} coefficient and the applied field, respectively, the magnitude of the outer fibre strain in a bimorph is

$$\varepsilon = \pm 1.5 E d_{31} \tag{1}$$

where E is the applied electric field across each layer embraced by an outer and inner electrode. This relationship can be used to simply calculate the actuated curvature in a straight bimorph. Since these structures are initially curved, more careful thought is required to determine the change of shape, as is now described.

Consider the curved bimorph in Fig. 1, with a mean radius of curvature R_m, thickness t and subtended angle α. For simplicity, the bimorph is planar since the width of structure into the page does not affect the degree of shape change but note that, in practice, it determines the limit on the applied loads. The d_{31} mode of actuation causes the structure to bend preferentially around the centre of curvature of the beam. In each layer between electrodes, there is also a d_{33} effect, which changes the thickness by approximately equal and opposite amounts. The net change in thickness is, therefore, zero. The change in length of the extreme fibres of the beam may therefore be expressed in terms of the radii before and after actuation:

$$(R_{m2} - t/2)\alpha_2 = (R_{m1} - t/2)\alpha_1(1 - \varepsilon) \tag{2}$$

$$(R_{m2} + t/2)\alpha_2 = (R_{m1} + t/2)\alpha_1(1 + \varepsilon) \tag{3}$$

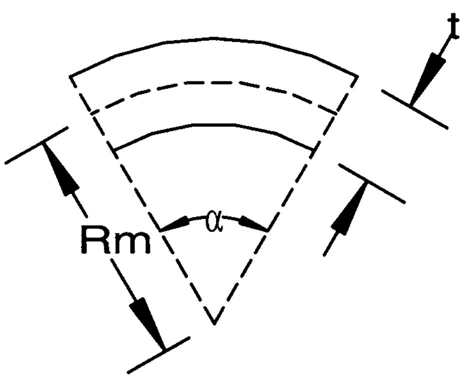

Figure 1 End view of an arbitrarily curved piezoelectric bimorph, of mean radius R_m, tape thickness t and subtended angle α.

where α_1 and α_2 are the unstrained and strained subtended angles. Using these relationships, the change in subtended angle, $\Delta\alpha$, can be readily derived

$$\Delta\alpha = \frac{2\alpha_1 \varepsilon R_m}{t} = \frac{3\alpha_1 E d_{31} R_m}{t} \tag{4}$$

It can also be assumed that the change in curvature does not promote an increase in arc-length of the neutral axis, positioned at the mean radius, thereby furnishing the following expression relating the mean radius and subtended angle to their respective changes

$$\Delta R_m = \frac{R_m \Delta\alpha}{\alpha_1 + \Delta\alpha} \tag{5}$$

The relationships in Equations 4 and 5 yield the unloaded actuation displacements in a curved structure with uniform section and include, for example, a simple open ring structure. However, the change in angle is limited, amongst other parameters, by the arc-length αR_m. Extra displacements may be gained by winding the structure to form multiple turns in one of two ways. First, if the structure has a small out-of-plane pitch angle, then it resembles a close-coiled helix of constant cylindrical radius: during actuation, the change in radius is constant, and the change in subtended angle along the axis of helix increases linearly with the number of turns. Second, the radius can be made to increase with subtended angle from the centre outwards, thus forming a spiral. If this rate of increase is small, then the actuation performance is approximately captured by the above. The product αR_m may be replaced by the total arc-length of section, L, and Equation 4 indicates that the change in subtended angle is therefore independent of the form of spiral to give

$$\Delta\alpha = \frac{3ELd_{31}}{t} \tag{6}$$

The manufacturing processes for the structures outlined above will be discussed later. Before proceeding, it is important to emphasise that there was assumed no change in through-thickness during actuation of the bimorph, as mentioned. However, this does not preclude the behaviour in other structures not necessarily of a bimorph lay-up. As a comparison, another derivation is now presented for a structure with no middle electrode and is based on a recent study of monolithic spiral-from piezoelectric devices [6].

In this case, the through-thickness strain is given by Ed_{33}, and the analysis considers the changes in radius of the extreme fibres due to a d_{31} effect, as before. The following relationships may now be stated

$$\frac{\Delta t}{t} = E d_{33} \tag{7}$$

$$\left.\frac{\Delta\alpha}{\alpha}\right|_N = -\frac{\Delta R}{R} \tag{8}$$

$$\left.\frac{\Delta\alpha}{\alpha}\right|_T = E d_{31} \tag{9}$$

where N and T indicate the normal and tangential directions relative to the surface of the curved section.

Summing the effects of the angular actuation from Equations 8 and 9 gives

$$\frac{\Delta\alpha}{\alpha} = E(d_{31} + d_{33}) \tag{10}$$

$$\frac{\Delta R}{R} = Ed_{33} \tag{11}$$

It is instructive to compare the change in subtended angles between monolithic and bimorph structures of the same thickness and initial radius: using Equations 10 and 4, and denoting with subscripts m and b, respectively, then

$$\frac{\Delta\alpha_b}{\Delta\alpha_m} = \frac{3d_{31}}{(d_{31} + d_{33})}\frac{R}{t} \tag{12}$$

For a typical piezoelectric composition, PZT-5H, which has coefficients $d_{33} = 593$ pC/N and $d_{31} = -274$ pC/N [7], the above relationship reduces to the simple formula

$$\frac{\Delta\alpha_b}{\Delta\alpha_m} = 2.6\frac{R_m}{t} \tag{13}$$

This indicates that a curved bimorph structure will usually undergo a greater bending actuation than a monolithic beam. This result may seem obvious, given that bimorphs deform in bending whereas in monolithic structures this may be an unforeseen result. However, there may be specific cases where a bimorph cannot be made or where a monolithic form may actually provide a better choice of actuator.

2. Experimental procedure

To test the theoretical predictions outlined above, piezoelectric spiral and helical bimorph forms were made. The technique used to fabricate these forms is a combination of various previously known manufacturing techniques. Firstly, the ceramic tape feedstock was formed using Viscous Processing, a technique described elsewhere [8, 9]. In this case, the binder system was chosen to be polyvinyl butyral and cyclohexanone. The de-agglomerated dough was extruded through an annular die of 0.8 mm width and 40 mm diameter, producing a tape of 125 mm in width. This tape was then calendered to the required thickness, which varied from 0.5 mm down to 100 microns. To protect the tape from drying, polyester sheet (Melinex) of 125 microns or 35 microns in thickness was applied by pressure rolling to both surfaces of the tape. Large quantities of feedstock could be made in this way, and stored for long periods without affecting the solvent content.

The bimorph structures were then produced via screen printing of the electrodes and laminating the sheets together. The internal electrode was first printed on to a pre-made tape, with one side of Melinex removed, the other remaining in order to protect the tape and to prevent distortion. After partial drying, this tape was laminated to another tape, using pressure rolling (and optionally applied heat). After this stage, each outer Melinex sheet was removed in turn, and the outer electrodes printed. A pure platinum ink was used for all the electrodes in this work, in order to achieve the best available properties and to minimise electrode/PZT interactions.

Strips of tape from the pre-printed and laminated sheets were then cut and wound into the required forms. For helical forms, a machined former was used to define the inner radius, and for the spirals, an interleaving layer of carbon tape was applied to obtain uniform separation of the turns. After drying at 50°C for several hours, the structures were subjected to standard binder removal and sintering schedules for this type of material (1°C/minute to 600°C; 10°C/minute to 1200°C, with a 1 hour hold). Example helical and spiral devices, in the green and sintered forms, are shown in Fig. 2. For the green spiral form, the carbon interleaving tape can be seen.

After sintering, soldered electrode contacts were made to the three separate electrodes in each case (inner, outer and internal). The devices were poled, while

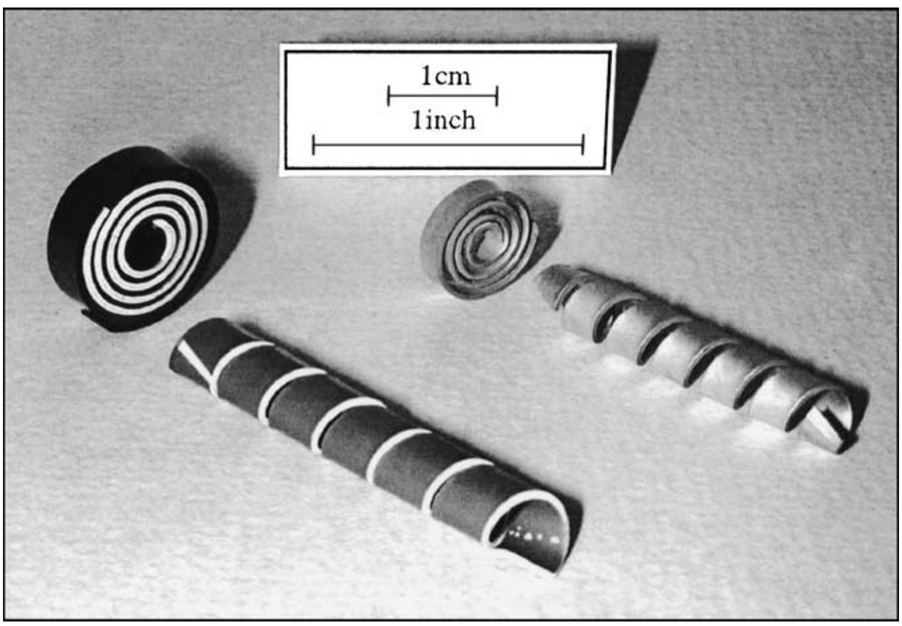

Figure 2 Piezoelectric bimorph helices and spirals in the green (left) and sintered forms.

being immersed in a heated silicone oil bath at between 120 and 130°C. Poling was performed by applying the positive terminal to the outer electrode and the inner to ground, with the internal electrode left unconnected. A voltage equivalent to a field of 2.5 kV/mm was applied across the tape for 10 minutes.

To measure the actuation behaviour, a laser displacement probe (Graham & White Instruments Ltd., UK, model M25) was used, together with a high voltage amplifier and a computer-controlled LavView-based system (National Instruments). The computer was used to generate a series of low frequency (5 Hz) and frequency-varying (5 to 400 Hz) inputs at differing voltage levels, in order to obtain the quasi-static and frequency response of the devices. The laser probe was positioned to read from a white planar surface bonded to the end of the helical or spiral device and aligned radially to magnify the rotational displacements. The linear measurement of the laser probe was then converted into a rotational reading, taking into account the significant twist of the measurement beam, using the following equation:

$$\Delta\alpha = \tan^{-1}\left(\frac{\delta}{R}\right) \tag{14}$$

where δ is the measured displacement, and R the radius at which the laser point is positioned.

To compare the effect of a monolithic versus bimorph beam, as calculated previously, two ways of actuating the devices were used. Firstly, the actuation voltage was applied across the inner and outer electrodes, ignoring the internal electrode, thus simulating a monolithic beam. Secondly, without changing the experimental set-up, the internal electrode was attached, and the two surface electrodes tied together to form a parallel bimorph arrangement. The results in terms of the peak-to-peak actuation versus the applied field as well as the frequency response of the actuators were then plotted.

3. Results and discussion

The variation is angular actuation as a function of frequency is shown in Fig. 3 for the test spiral in both monolithic and parallel bimorph modes, the dimensions of which are given in Table I. The electric field was kept constant in both cases, equivalent to 30 V/mm peak. The basic resonant nature of the device is unchanged, though the value of the resonant frequency is reduced for the bimorph-driven mode. This reduction is due to the non-linear elastic behaviour of the material, which reduces the effective material stiffness at higher strains. The large increase in actuation efficiency for the device being driven as a bimorph rather than a monolithic structure is evident. The difference at low frequency in this case was found to be approximately 10 times. For a spiral structure, the relationship given in Equation 13 cannot be used to give an exact prediction, since the spiral radius is not constant. However, given the fact that the spiral radius varies between 1.85 and 5 mm from inner to outer turns, with a constant tape thickness of 0.5 mm, Equation 13 would predict a factor of between 10 and 26. This appears to suggest that the difference between the two modes of actuation is in practice not as large as that suggested by the model.

To measure more accurately the effect of bimorph versus monolithic mode curved structures, a constant value for the radius and tape thickness is required, which is given by a helical rather than spiral geometry. The results from a test helix, the dimensions of which are given in Table I, in terms of the angular actuation response as a function of electric field, driven at a constant frequency of 5 Hz, are given in Fig. 4 for the monolithic

TABLE I Geometries of the spiral and helical devices tested

	Tape thickness (t/mm)	Tape width (w/mm)	Number of active turns N	Mean radius (R_m/mm)	Tape length (L/mm)
Spiral:	0.5	2.0	3.5	–	80
Helix:	0.65	3.5	7.5	2.0	100

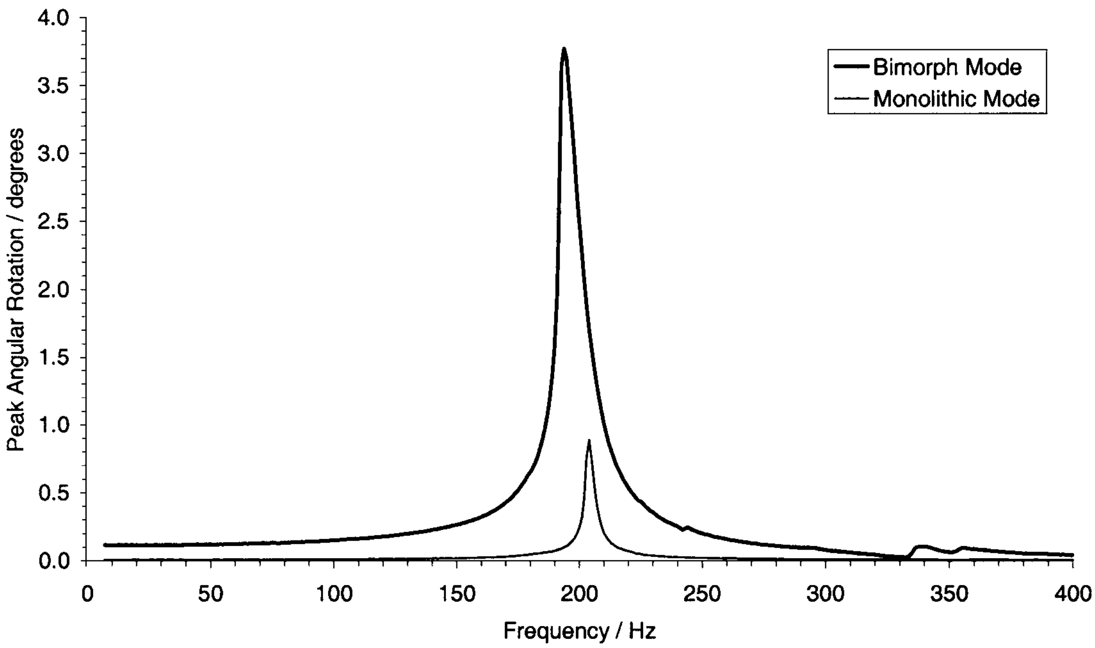

Figure 3 Rotational behaviour as a function of frequency for a piezoelectric spiral in monolithic and bimorph modes.

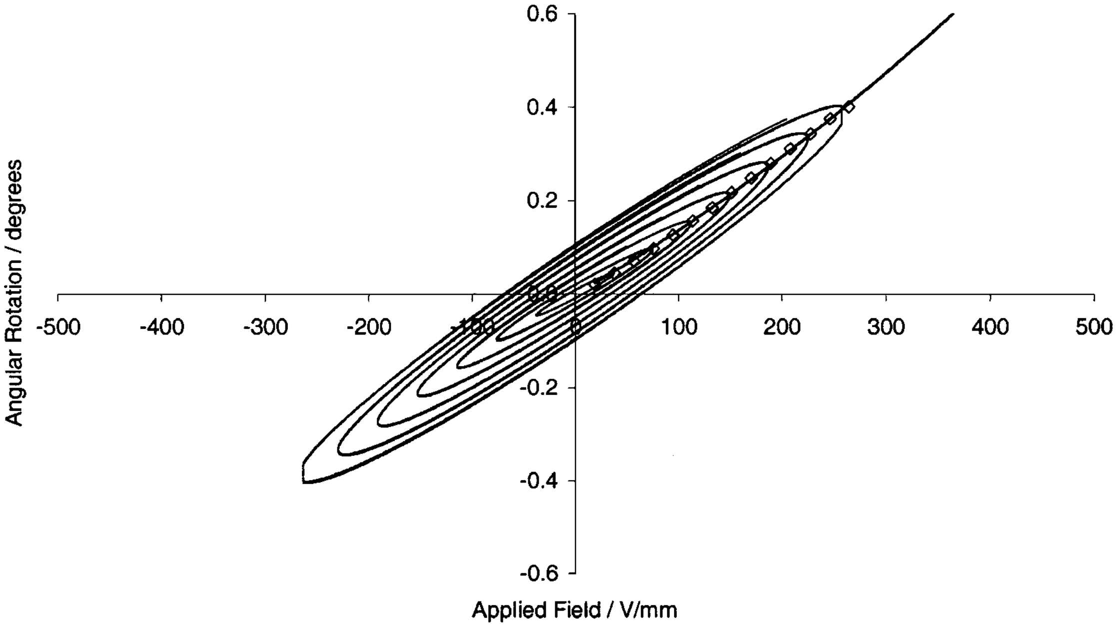

Figure 4 The effect of electric field amplitude on the angular actuation response of a piezoelectric helical bimorph, driven in monolithic mode.

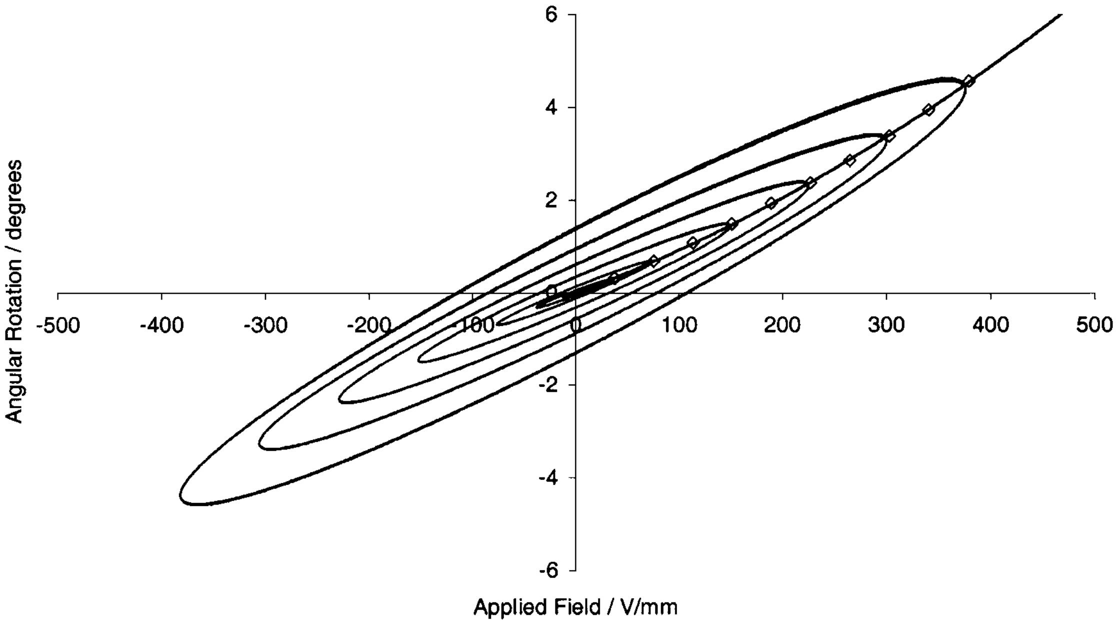

Figure 5 The effect of electric field amplitude on the angular actuation response of a piezoelectric helical bimorph, driven in parallel bimorph mode.

mode and in Fig. 5 for the bimorph mode. Again, the large difference between the two driven modes is clear. For this particular helix, with the dimensions given in Table I, Equation 14 predicts a factor of 7.93. The theory assumes linearity of response, which may account for at least some of the discrepancy of behaviour of actuation. To remove the non-linear effects, the curve described by the peak angular response versus the applied field can be accurately fitted to a simple quadratic equation, described by the function

$$\Delta\alpha = AE + BE^2 \quad (15)$$

where $\Delta\alpha$ is degrees, and E is in V/m. The two constants for the monolithic and bimorph modes, derived from the data shown in Figs 4 and 5, are given in Table II.

TABLE II Theoretical versus experimental results for the test helix driven in monolithic and bimorph modes

	$A/\times10^{-3}$ °mm/V	Linear $\Delta\alpha$ at $E = 500$ V/mm	$B/\times10^{-6}$ °mm/V	Total $\Delta\alpha$ at $E = 500$ V/mm
Monolithic mode experimental	1.26	0.63°	1.06	0.89°
Monolithic mode theoretical	–	0.43°	–	0.43°
Bimorph mode experimental	8.23	4.11°	9.83	6.57°
Bimorph mode theoretical	–	3.41°	–	3.41°
$\Delta\alpha_b/\Delta\alpha_m$ experimental		6.53		7.38
$\Delta\alpha_b/\Delta\alpha_m$ theoretical		7.93	–	7.93

The magnitude of the angular actuation can also be compared to that predicted by the theoretical derivation, namely the result of Equation 4. For the helix in question, the value for α is given by $2\pi N$, where N is the number of 'active' turns, i.e., the number of turns between the mounting points. The results comparing the experimental data with the theoretical predictions (based on the standard properties of PZT-5H given previously) are also outlined in Table II. For both the monolithic and bimorph modes, the experimental data, even allowing for the non-linear response of the material, shows a large increase over that predicted. For the bimorph mode, this is around 20%, and for the monolithic mode it is over 45%. Various causes can be attributed to these discrepancies. The first is the uncertain value of the d_{31} and d_{33} constants, which are often quoted by manufacturers to be within ±10% tolerances [7]. However, the value for d_{31} indicated by the bimorph mode result is 330 pC/N, which is well beyond these limits. Secondly, the theory assumes that the behaviour of the bimorph device is similar to that of a planar bimorph, i.e. the same type and change of curvature occurs. This may not be the case, since the tape thickness is significant compared to the initial curvature in this case. Thirdly, the theory does not take into account the fact that the device is 3-dimensional, but merely extrapolates the behaviour of a 2-dimensional beam. Since the initial curvature of the helix causes the bending stiffness of the tape to be much greater across the tape width than around the axis of the helix or spiral, it results in a preferred mode of bending, which could increase the measured actuation for a given field. All these possible causes may be investigated in further work, through careful experiments to isolate them individually. For example, the piezoelectric coefficients could be confirmed with measurements on planar bimorphs made with the same processing route. Secondly, the effect of tape thickness to radius of curvature may be addressed by measuring the effect on angular actuation for a series of curved structures using the same tape length, width and thickness but with varying radii. Finally, the 3-dimensional effects may be addressed using more complex analytical and computer-aided modelling.

4. Conclusions

It has been shown clearly that net shape-formed piezoelectric bimorph spirals and helices can be made, and can generate large static rotational actuation displacements, in this case of up to several degrees. The processing route employed to make these structures has proved to be highly flexible and efficacious in generating various kinds of shapes which require a plastic green forming stage in addition to co-fired electrodes. Such devices have previously not been made via any known route.

The efficiency of actuation for bimorph forms is greatly increased over the monolithic equivalent. The improvement in actuation responses in the devices made thus far has been predicted and measured. The bimorph-actuated helical device has been shown to be up to 7 times more active than the equivalent monolithic structure, in terms of the actuation response versus applied field. The particular spiral geometry investigated has shown an improvement of up to 10 times over the monolithic mode.

The theoretical predictions for the helical geometry device have so far underestimated the actual responses by 20% in the case of the bimorph mode and over 40% for the monolithic mode. Various possible reasons for this discrepancy have been proposed, and these will be the subjects of further research.

Further work is being directed towards practical actuators utilising the novel modes possible with spiral and helical form piezoelectric bimorphs. The rotational actuations achieved thus far show a great deal of promise for static or dynamic positioning, and various acoustic applications. More investigations need to be carried out in order to improve understanding of the behaviour of these novel devices.

Acknowledgements

This work was funded with support from a European Union Framework V grant [G1RD-CT-1999-00121] and from 1...Limited, Cambridge.

References

1. G. H. HAERTLING, *J. Amer. Ceram. Soc.* **82**(4) (1999) 797.
2. T. OHBA and H. KOGA, US Patent no. 4441128 (1984).
3. H. H. KOLM and E. A. KOLM, US Patent no. 4435667 (1984).
4. R. ADLER, US Patent no. 3900748 (1975).
5. A. J. MOULSON and J. M. HERBERT, in "Electroceramics" (Chapman and Hall, London, 1990) p. 298.
6. F. MOHAMMADI, A. L. KHOLKIN, B. JADIDIAN and A. SAFARI, *App. Phys. Lett.* **75**(16) (1999) 2488.
7. "Data Book for Engineers" (Morgan Electroceramics, Southampton, 2000).
8. N. ALFORD, J. D. BIRCHALL and K. KENDAL, *Nature* **330**(6143) (1987) 51.
9. D. H. PEARCE, G. DOLMAN, P. A. SMITH and T. W. BUTTON, in Proc. Electroceramics V (1996) Vol. 2, p. 385.

Received 3 June 2001
and accepted 10 January 2002